Pharm Res (2011) 28:1919–1930
DOI 10.1007/s11095-011-0419-4

RESEARCH PAPER

Laser-Engineered Dissolving Microneedle Arrays for Transdermal Macromolecular Drug Delivery

Katarzyna Migalska • Desmond I. J. Morrow • Martin J. Garland • Raj Thakur • A. David Woolfson • Ryan F. Donnelly

Received: 13 December 2010 / Accepted: 4 March 2011 / Published online: 25 March 2011

ABSTRACT

Purpose To assess the feasibility of transdermal macromolecule delivery using novel laser-engineered dissolving microneedles (MNs) prepared from aqueous blends of 20% *w/w* poly (methylvinylether maleic anhydride) (PMVE/MA) *in vitro* and *in vivo*.

Methods Micromoulding was employed to prepare insulin-loaded MNs from aqueous blends of 20% *w/w* PMVE/MA using laser-engineered moulds. To investigate conformational changes in insulin loaded into MNs, circular dichroism spectra were obtained. *In vitro* drug release studies from MNs across neonatal porcine skin were performed using Franz diffusion cells. The *in vivo* effect of MNs was assessed by their percutaneous administration to diabetic rats and measurement of blood glucose levels.

Results MNs loaded with insulin constituted exact counterparts of mould dimensions. Circular dichroism analysis showed that encapsulation of insulin within polymeric matrix did not lead to change in protein secondary structure. *In vitro* studies revealed significant enhancement in insulin transport across the neonatal porcine skin. Percutaneous administration of insulin-loaded MN arrays to rats resulted in a dose-dependent hypoglycaemic effect.

Conclusion We demonstrated the efficacy of MNs prepared from aqueous blends of PMVE/MA in transdermal delivery of insulin. We are currently investigating the fate of the delivered insulin in skin and MN-mediated delivery of other macromolecules.

K. Migalska • D. I. J. Morrow • M. J. Garland • R. Thakur • A. D. Woolfson • R. F. Donnelly (✉)
School of Pharmacy, Queen's University Belfast,
Medical Biology Centre,
97 Lisburn Road,
Belfast BT9 7BL, UK
e-mail: r.donnelly@qub.ac.uk

KEY WORDS insulin · laser engineering · microneedles · transdermal drug delivery

ABBREVIATIONS

BGL	blood glucose level
BSA	bovine serum albumin
CD	circular dichroism
MN	microneedle
PMVE/MA	poly(methylvinylether) maleic anhydride
SC	*stratum corneum*

INTRODUCTION

Development of sophisticated biotechnological methods now allows for production of large quantities of peptide/protein molecules at a lower cost and in a relatively easy manner, as well as production of modified proteins with improved physiological characteristics (1). As proteins and peptides differ in respect to biochemistry and structure from conventional low molecular weight, organic pharmaceuticals, a number of challenges have to be addressed, and unique requirements have to be satisfied in order to successfully deliver peptide/protein-based therapeutics to their site of action (2). The skin is an appealing site for the systemic delivery of pharmaceuticals (3,4). The transdermal route offers certain advantages among other non-invasive routes of drug delivery, such as avoidance of first-pass hepatic metabolism and potential for continuous drug administration. With respect to peptide/protein delivery, the lower proteolytic activity of the skin in comparison to other routes of administration is also favourable (5). However, peptides and proteins, as large and hydrophilic molecules, do not have the ability to passively permeate

across the principal barrier of the skin, the *stratum corneum* (*SC*). Therefore, a wide range of strategies aimed at facilitating peptide/protein transdermal delivery are currently under investigation, such as iontophoresis, electroporation, ultrasound, laser poration and thermal ablation (6–10).

Microneedles are micron-scale devices capable of circumventing the *SC* barrier and allowing for improved percutaneous transport of drugs (11). Application of MNs to the skin has been demonstrated to be painless (12). Delivery of a wide range of therapeutics across the skin with the aid of MNs has been achieved *via* four main strategies: 1) 'poke-with-patch' approach involves application of a solid MN array to create micropores followed by removal of the array and administration of the drug formulation in the form of a transdermal patch, gel or solution (13,14); 2) 'coat-and-poke' approach relies on coating the drug formulation onto the microprojections and insertion of the MN array into the skin (15); 3) 'poke-and-flow' approach involves use of hollow MNs to inject liquid drugs into the skin (16); 4) 'poke-and-release' approach involves incorporation of drug molecules into the structure of polymeric, biodegradable MNs and subsequent insertion into skin (17,18). Each of these approaches is associated with certain advantages and limitations. Polymeric MNs are an attractive option for delivery of drug molecules across the skin. First, in contrast to silicon, which is not an FDA-approved material, a wide range of polymers are known to be biocompatible and have long safety records (19). The use of water-soluble and biodegradable polymers eliminates the risk of leaving biohazardous sharp waste in the skin and guarantees safe MN disposal by mechanical destruction or dissolution in a solvent (19,20). In addition, the low cost of polymeric materials and their easy fabrication by micro-moulding processes allows for mass MN production. However, in the case of polymeric MNs, drug loading can compromise their mechanical strength, and the fabrication process can have an influence on the stability of incorporated molecules.

We have previously proposed a novel laser-based method for micro-moulding of MN arrays from polymeric materials under ambient conditions. The avoidance of drug exposure to harsh conditions (e.g. elevated temperature) is a distinct advantage and allows for application of this manufacturing technique to fabricate MNs encapsulating peptides/proteins in their structure for rapid delivery (21). In addition, MN arrays with different geometries can be easily fabricated, providing the ability to manipulate dosing profiles by changing number and length of the needles. Moreover, we demonstrated that aqueous blends of 20% *w/w* PMVE/MA formed MNs that showed superior mechanical strength and stability at ambient conditions in comparison to other materials tested. These MNs significantly enhanced percutaneous delivery of the low molecular weight drug theophylline (21). The current study aims to establish the usefulness of MNs prepared from aqueous blends containing 20% *w/w* PMVE/MA to deliver peptides/proteins across the skin. Insulin was selected as a model macromolecule, due to its clinical relevance.

MATERIALS AND METHODS

Chemicals

Gantrez® AN-139, a copolymer of methylvinylether and maleic anhydride (PMVE/MA) was provided by ISP Co. 120 Ltd., Guildford, UK. Insulin from bovine pancreas, 27 USP IU/mg, was obtained from Sigma Aldrich, Dorset, UK. Isoflurane inhalation anaesthetic was obtained from Abbott Laboratories Ltd., Kent, UK. All other chemicals used were of analytical reagent grade.

Fabrication of Insulin-Loaded MNs Prepared from Aqueous Blends of 20% *w/w* PMVE/MA

MNs prepared from aqueous blends of 20% *w/w* PMVE/MA and loaded with insulin were prepared using laser-engineered silicone micromould templates, as described previously (21). Briefly, silicone elastomer was poured into a custom-made aluminium mould and cured overnight at 40°C. A laser-machine tool (BluLase® Micromachining System, Blueacre Technology, Dundalk, Ireland) with a laser (Coherent Avia, Coherent Inc., Pittsburgh, USA) emitting a beam having a wavelength of 355 nm and a pulse length of 30 ns (variable from 1 to 100 kHz) was then employed to produce MN moulds (11×11 array, 600 μm height, 300 μm width and 300 μm interspacing at MN base). A 30% *w/w* aqueous solution of PMVE/MA was prepared by adding the required mass of PMVE/MA to ice-cold deionised water, followed by vigorous stirring and heating at 95.0°C until a clear gel was obtained, due to hydrolysis of the anhydride form of the copolymer to the corresponding acid. Upon cooling, the blend was then readjusted to the final concentration of 30% *w/w* by addition of an appropriate amount of deionised water. To prepare insulin-loaded MNs, the stock solution was diluted with the appropriate amount of 0.01 M HCl in which the amount of insulin necessary to obtain 2.5 mg and 10 mg loadings per device was dissolved. This solution was then poured into the silicone micromould, centrifuged for 15.0 min at 3500 rpm and allowed to dry under ambient conditions for 24 h.

Measurement of MN Fracture Force

The effect of insulin loading on MN strength was assessed as described previously (21). In brief, an axial compression load was applied to the MN arrays using a TA.XT-plus Texture Analyser (Stable Micro Systems, Surrey, UK). MN arrays were attached to the moving testing probe of the Texture Analyser using double-sided adhesive tape. The test station pressed MN arrays against a flat block of aluminium with three different forces: 0.05, 0.36 and 0.71 N/needle for 30 s, at a rate of 0.5 mm/s. Pre-test and post-test speeds were 1 mm/s, and the trigger force was 0.049 N. Before and after fracture testing, all MNs of each array were visualised using a light microscope (GXMGE-5 USB Digital Microscope, Laboratory Analysis Ltd., Devon, UK). The height of the MNs before and after testing was measured using the ruler function of the microscope software so that the percentage change in the MN height could be calculated.

Determination of Insulin Secondary Structure by Circular Dichroism (CD)

To examine the secondary structure of insulin after encapsulation and release from dissolving MNs, CD was employed. CD spectra were obtained with a Jasco J-185 spectropolarimeter equipped with a temperature controller. CD spectra were collected at 20°C using a 1 cm quartz cell over the wavelength range of 200–400 nm. A resolution of 0.1 nm and scanning speed of 200 nm/min were employed. Samples for CD analysis were prepared by dissolution in 0.01 M HCl. The spectra of insulin samples with concentrations of approximately 0.025 mg/ml were compared with that of fresh insulin in 0.01 M HCl.

In Vitro Insulin Permeation Studies

Diffusion of insulin (M_w 5.6 kDa) from polymeric MN arrays across neonatal porcine skin was investigated *in vitro* using modified Franz diffusion cells (FDC-400 flat flange, 15 mm orifice diameter, mounted on an FDCD diffusion drive console providing synchronous stirring at 600 rpm and thermostated at 37±1°C) (Crown Glass Co. Inc., Somerville, NJ, USA). Receptor compartment volumes, approximately 12 ml, were exactly determined by triplicate measurements of the weights of water they could accommodate. Neonatal porcine skin was obtained from stillborn piglets and immediately (<24 h after birth) excised, trimmed to a thickness of 300±50 μm using dermatome and frozen in liquid nitrogen vapour. Skin was then stored at −20°C until further use. Shaved skin samples were pre-equilibrated in receptor medium, 0.1 M Tris buffer pH 10 for 1 h before beginning of the experiments. A circular specimen of the skin was secured to the donor compartment of the diffusion cell using cynoacrylate adhesive (Loctite, Dublin, Ireland) with the *stratum corneum* side facing the donor compartment. Using the applicator, MNs were inserted with an application force of 4.4 N/array into the centre of the skin. MNs were kept in place during the experiment by application of a non-adhesive putty material (BluTac®, Bostik Ltd., Leicester, UK) to their upper surface. With MN arrays in place, donor compartments were mounted onto the receptor compartments of the Franz cells. Using a long needle, samples (0.30 ml) were removed from the receptor compartment at defined time intervals and replaced with an equal volume of 0.1 M Tris buffer pH 10. Sink conditions were maintained throughout the experiment. The concentrations of insulin in the receiver medium were determined by HPLC analysis, as described below.

Pharmaceutical Analysis of Insulin

Insulin analysis was performed using RP-HPLC (Agilent 1200® Binary Pump, Agilent 1200®, Standard Autosampler, Agilent 1200® Variable Wavelength Detector, Agilent Technologies UK Ltd., Stockport, UK) with UV detection at 214 nm. Gradient separation was achieved using an RP C_4 (4.6 mm×50 mm, 5 μm packing) Symmetry300 (Waters Associates, UK) analytical column. The mobile phase gradient consisted of ACN and 0.1% *v*/*v* trifluoroacetic acid (TFA) aqueous solution. The gradient linearly changed from 25:75 (ACN:TFA) to 35:65 in 5 min followed by a 3 min isocratic 35:65 ratio and a 7 min re-equilibration period. The injection volume was 20 μl, and elution was at a flow rate of 0.6 ml/min. The chromatographs obtained were analysed using Agilent ChemStation® Software B.02.01. Least squares linear regression analysis and correlation analysis were performed on the calibration curve produced, enabling determination of the equation of the line, its coefficient of determination and the residual sum of squares (R*SS*). To determine limit of detection (*LoD)* and limit of quantification (*LoQ*), an approach based on the standard deviation of the response and the slope of the representative calibration curve was employed, as described in the guidelines from ICH (44). The *LoD* of a chromatographic method was determined as follows, using Eq. 1:

$$LoD = \frac{3.3\sigma}{S} \tag{1}$$

where σ is the standard deviation of the response (peak area) of the data used to construct the regression line and S is the slope of that line. Similarly, the *LoQ* was determined using Eq. 2:

$$LoQ = \frac{10\sigma}{S} \tag{2}$$

In Vivo Evaluation of the Efficacy of Dissolving MNs Prepared from Aqueous Blends of 20% *w/w* PMVE/MA for Transdermal Delivery of Insulin

Sprague–Dawley male rats weighing 264 ± 13 g were used. The animals were acclimatized to laboratory conditions for 7 days before the experiment. All animal experiments throughout this study were conducted according to the policy of the federation of European Laboratory Animal Science Associations and the European Convention for the Protection of Vertebrate Animals used for Experimental and Other Scientific Purposes, with implementation of the principle of the 3Rs (replacement, reduction, refinement). This research also adhered to the "Principles of Laboratory Animal Care" (NIH publication 85–23, revised in 1985).

Diabetes was induced by a single intraperitoneal injection of streptozotocin (65 mg/kg) in 0.1 M citrate buffer pH 4.6. Two to four days after injection, blood glucose levels (BGL) were determined using glucometer (Accu-Check® Aviva, Roche Ltd., Mannheim, Germany) to ensure that diabetes had been induced. Animals with BGL above 20 mmol/l were considered diabetic and were included in the study. To prevent fur from interfering with dermal contact of the patch, animals were anesthetized using gas anaesthesia (2–4% isoflurane in oxygen) 24 h before experimentation, and the hair was removed with an animal hair clipper. Additionally, depilatory cream (Boots Expert®, The Boots Company PLC, Nottingham, U.K.) was used to remove any residual hair. Prior to the experiments, animals were fasted for 12 h with free access to water. Animals were fasted for further 12 h throughout the experiment. Positive controls were performed by subcutaneously injecting bovine insulin solution in PBS pH 7.4 at a dose of 0.2 IU per animal. MN arrays were manually inserted into the skin at a site on the rat's back. After application of MN arrays, blood samples were collected at different time points over a 12 h period by lateral tail vein prick and BGL were measured using a glucometer. As a negative control for dissolving PMVE/MA MNs experiments, insulin-loaded MN baseplates were applied to the rats. In addition, in order to evaluate if the biological activity of insulin encapsulated in MN matrix was retained, insulin extracted from MNs was subcutaneously injected at a theoretical dose of 0.2 IU per animal into diabetic rats. MN arrays prepared from aqueous blends of 20% *w/w* PMVE/MA and loaded with 10 mg and 2.5 mg insulin were dissolved in 0.01 M HCl and further diluted to a concentration of 0.2 IU/ml in PBS pH 7.4 just before administration. The volume of 1 ml of the obtained solutions was subcutaneously administered to rats. Blood glucose levels were expressed as the percentage of initial blood glucose levels, and calculated values were plotted against time to obtain blood glucose level-time profiles. C_{max} denoting maximum percentage decrease in blood glucose levels was calculated by subtracting the lowest percentage blood glucose level from 100, as described elsewhere (47). T_{max} denoting the time required to achieve C_{max} was also reported (47).

RESULTS

MNs prepared from aqueous blends containing 20% *w/w* PMVE/MA and loaded with 2.5 mg and 10 mg insulin per array were fabricated using silicone laser-engineered moulds. Visual inspection of manufactured MNs revealed that incorporation of insulin into the polymeric matrix of the MNs did not result in any changes in MN morphology, as can be appreciated from Fig. 1. The effect of insulin encapsulation on mechanical strength of MNs was assessed. Figure 2 depicts the result from the investigation of the effect of insulin loading on the degree of damage being caused to the MNs upon exertion of an increasing axial load. Reduction in the height of the MNs was found to increase with the load applied. Simultaneously with the compression, MN tips were bent up to 90° to one side. There was no significant difference observed in the degree of deformation between MNs without insulin and MNs encapsulating 2.5 mg and 10 mg of insulin at any of the axial forces applied ($p > 0.05$ in each case).

Table I shows calibration curve properties for the insulin analytical method. The retention time of insulin monomer was approximately 5 min. The calibration curve was found to be linear in the range of 0.001–0.025 mg/ml. The developed HPLC assay for determination of insulin monomer was found to be reproducible, with good precision and accuracy (Table II). The method specificity investigations revealed that under the assay conditions described above no interference from the microneedle matrix was observed. The preliminary studies of insulin stability in solution under exposure to potentially destabilizing conditions (agitation at 600 rpm at 32°C and the

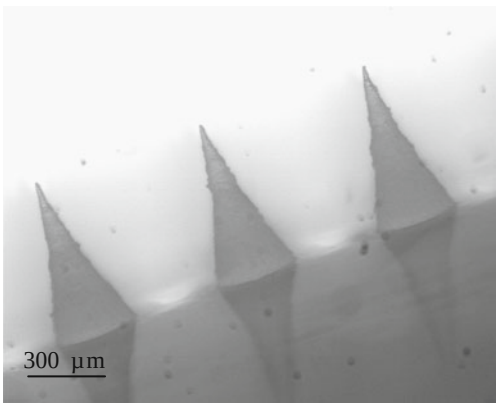

Fig. 1 Representative digital microscope image of MNs prepared from aqueous blends of 20% *w/w* PMVE/MA and loaded with 10 mg insulin.

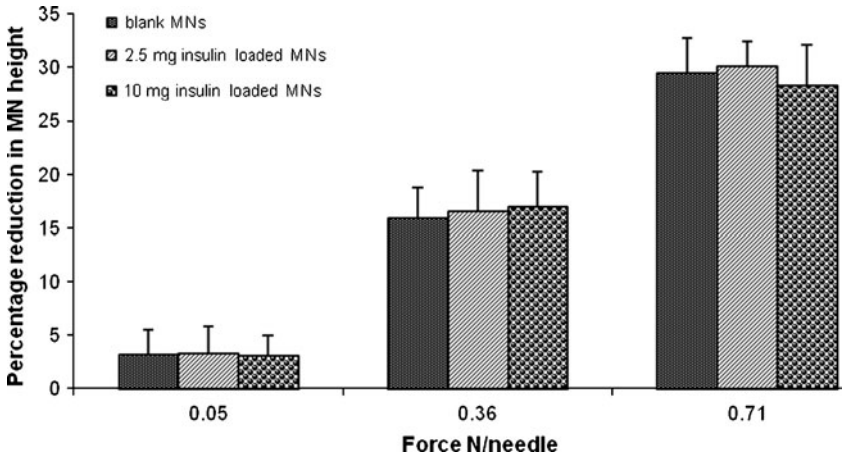

Fig. 2 Percentage reduction in the height of MNs following the application of an increasing axial load (means ± SD, $n = 45$).

presence of hydrophobic and hydrophilic surfaces) indicated its instability in PBS pH 7.4. None of the additives employed to stabilize insulin monomer, i.e. urea, ascorbic acid, glycerol, n-octyl-β-glucopyranoside, sodium dodecyl sulphate, were effective. No insulin loss was observed in 0.1 M Tris buffer pH 10; therefore, this buffer was selected as a release medium for *in vitro* release experiments. It could be hypothesised that improved stability of insulin at higher pH was related to its self-association state. Kadima *et al.* (1993) suggested that at pH 10 insulin monomer carries six negative charges in comparison to just two at pH 7.5 (45). Therefore, electrostatic repulsions between insulin monomers are more pronounced at higher pH, which prevents self-association into hexamers and favours presence of the monomeric species. Similar findings were reported by Tokumoto *et al.* (2006) during evaluation of the effect of electoporation and pH on iontophoretic *in vivo* percutaneous adsorption of human insulin. Tokumoto *et al.* (2006) explained that the much higher plasma levels observed when the pH of insulin solution was increased from 7 to 10, after combined use of electoporation and iontophoresis, were caused by the different self-association properties of insulin at pH 7 and pH 10. The results from the investigations of insulin self-association revealed that at pH 10, insulin monomers and dimers were observed in addition to hexamers, whereas most of the insulin was in the hexamer form at pH 7 (46).

Table III presents the results obtained during insulin content analysis by RP-HPLC. Content analysis revealed that 93.6% and 94.5% of insulin incorporated at a theoretical amount of 2.5 mg and 10 mg per array was recovered from MN arrays dried for 24 h at room temperature (0 days), respectively. Statistical analysis showed that there was no significant difference between content of 2.5 mg and 10 mg insulin-loaded MN arrays after 7 and 28 days of storage at room temperature, in comparison to the insulin amount recovered at 0 days ($p > 0.05$ in all cases). Insulin content in the needles only was found to be 0.05 mg (1.35 IU) and 0.29 mg (7.83 IU) for 2.5 mg and 10 mg loaded MN arrays, respectively.

Any conformational changes in the insulin secondary structure upon encapsulation within the PMVE/MA matrix were investigated using CD spectroscopy. Figure 3 represents circular dichroism spectra of insulin after incorporation and release from MNs prepared from aqueous blends of 20% *w/w* PMVE/MA. The CD spectrum of insulin standard solution shows a strong negative minimum at 208 and less pronounced minimum at 222 nm. These bands are indicative of typical alpha-helical structure (22,23). CD spectra of insulin incorporated into the MN matrix at both loadings, 2.5 and 10 mg per array, were almost identical to that of insulin standard solution, indicating that no changes in the secondary structure of insulin were incurred during encapsulation in MNs.

Figure 4 illustrates the permeation profiles of insulin released from MNs prepared from aqueous blends of 20% *w/w* PMVE/MA across dermatomed neonatal porcine skin. Insulin did not permeate across neonatal porcine skin when MN base-plates were tested. When 2.5 mg and 10 mg insulin-loaded MN arrays were used, insulin delivery was significantly increased in comparison to the negative control after 24 h of the investigation ($p < 0.05$ in both cases). The study revealed that insulin release from the MN matrix showed a burst effect within the first 15 min of the experiment. However, the initial burst effect was not followed by a significant further increase in the amount of insulin delivered during the remaining part of the study.

Table I Calibration Curve Properties of Insulin as Determined by Linear Regression and Correlation Analysis and *LoD* and *LoQ*

Slope	y-Intercept	r^2	RSS	*LoD* (μg/ml)	*LoQ* (μg/ml)
280.03	−88.26	0.9986	59624.43	0.77	2.33

Table II Assay Variability for Determination of Insulin by HPLC

Selected concentration (μg/ml)	Mean concentration found (μg/ml)	SD	CV (%)	Accuracy (%)
Intraday				$n=4$
10	9.70	0.23	2.36	97.03
15	15.00	0.44	2.96	100.00
20	20.34	0.31	1.52	101.68
Inter day				$n=3$
10	9.68	0.26	2.73	96.84
15	15.58	0.32	2.04	103.85
20	20.84	0.22	1.04	104.18

The cumulative amount of insulin delivered across neonatal porcine skin after 24 h from 10 mg and 2.5 mg loaded MN arrays was approximately 161 μg and 20 μg, respectively, which accounted for approximately 55% and 40% of the actual insulin loading in the needles. Therefore, *in vitro* permeation experiments across skin indicated that, most probably, only insulin present in the needles, not MN baseplates, was delivered.

Figure 5(a–c) shows the representative digital images of Franz cell donor compartment (a), insulin-loaded MN array (b) and *SC* side-up dermatomed porcine skin (c) after 24 h from the start of experiment. No visible MN puncture holes were observed on the dermal side of dermatomed porcine skin at the end of the release study (Fig. 5a). After removal of dermatomed porcine skin from the Franz cell donor compartment, it was found that no needles were present and the MN array was completely dissolved (Fig. 5b). MN puncture holes were not visible on the *SC* side of the dermatomed porcine skin at the end of the 24 h experimental period (Fig. 5c).

In order to evaluate if the pharmacological efficacy of insulin incorporated into MN arrays was preserved, decrease in BGL as a biological response to the administration of insulin was determined. Figure 6 shows the hypoglycaemic effect induced by subcutaneous administration of insulin released from dissolved MN arrays in comparison to subcutaneous administration of freshly prepared 0.2 IU/ml insulin solution. It was observed that administration of insulin released from dissolved 2.5 mg and 10 mg loaded MN arrays resulted in a hypoglycaemic effect. Table IV presents the pharmacodynamic parameters: C_{max} and T_{max} of insulin recovered from PMVE/MA MN arrays and subcutaneously administered to diabetic rats. In addition, C_{max} and T_{max} parameters of subcutaneously administered freshly prepared insulin solution are presented. In the rats that received insulin solutions recovered from 2.5 mg loaded MN arrays, the BGL had decreased by 60% from the initial value within 2 h of administration. A maximum reduction in BGL by approximately 92% was observed after 4.4 h from the injection, and BGL returned to the baseline after approximately 12 h. Administration of insulin solution released from 10 mg loaded MN arrays led to a similar hypoglycaemic response. However, the drop in BGL was slower in the beginning, and, after 2 h, a reduction by approximately 36% was observed. After 4 h from the onset of the experiment a maximum fall in BGL of approximately 77% was recorded, and that value returned to the initial BGL after approximately 10 h. When freshly prepared insulin solution was administered, after 2 h, BGL dropped by approximately 78%, and a maximum reduction in BGL by approximately 85% was observed after 2.7 h from the beginning of the experiment. BGL returned to the initial value after approximately 6 h. Statistical analysis revealed that there was significant difference in the mean C_{max} values induced by administration of insulin released from 2.5 mg loaded MN arrays in comparison to C_{max} produced by the administration of fresh insulin solution ($p<0.05$). However, no statistically significant difference was observed between the mean C_{max} values induced by administration of insulin released from 10 mg loaded MN arrays in comparison to C_{max} produced by the administration of fresh insulin solution ($p>0.05$). Statistically significant difference was observed between T_{max} of insulin recovered from 2.5 mg and 10 mg loaded MNs and subcutaneously administered to diabetic

Table III Determination of Insulin Content in MN Arrays at Different Time Points by the RP-HPLC Method (Means ± SD, $n=5$)

Insulin loading (mg/array)	Recovery			
		0 day	7 days	28 days
2. 50	mg	2.34 ± 0.09	2.26 ± 0.19	2.20 ± 0.08
	%	93.61 ± 3.54	90.21 ± 7.48	87.90 ± 3.15
10.00	mg	9.45 ± 0.20	9.39 ± 0.41	9.27 ± 0.28
	%	94.45 ± 2.00	93.91 ± 4.12	92.68 ± 2.78

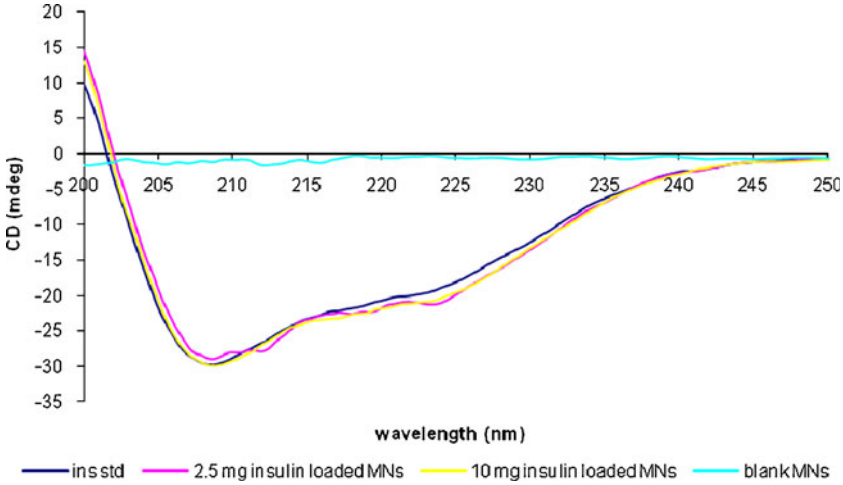

Fig. 3 CD spectra of insulin encapsulated and released from MNs prepared from aqueous blends of 20% *w/w* PMVE/MA at a loading of 2.5 mg per array (*pink*), 10 mg per array (*yellow*) and CD spectra of insulin standard solution (*dark blue*) and non-insulin loaded MNs (blank MNs) (*light blue*).

rats in comparison to T_{max} of freshly prepared insulin solution ($p<0.05$ in both cases).

Administration of insulin by application of MN base-plates loaded with 2.5 mg and 10 mg insulin did not result in a hypoglycaemic effect in diabetic rats. Blood glucose levels remained relatively unchanged during the experimental period, which could suggest that hair removal procedures did not affect skin barrier function. Figure 7 represents BGL *versus* time profiles obtained after application of 2.5 mg and 10 mg insulin-loaded MNs and placebo (no insulin) MNs prepared from aqueous blends of 20% *w/w* PMVE/MA to diabetic rats. The results revealed that administration of insulin *via* the transdermal route by means of MN arrays prepared from aqueous blends of 20% *w/w* PMVE/MA resulted in a hypoglycaemic effect. No reduction in BGL was observed when placebo MN arrays were transdermally applied to diabetic rats. Table V presents the pharmacodynamic parameters, C_{max} and T_{max} of insulin transdermally delivered with MN arrays to diabetic rats. Administration of 2.5 mg insulin-loaded MN arrays induced a slight hypoglycaemic effect in diabetic rats. A maximum drop in BGL by approximately 32% was observed after 2.7 h from the onset of MN array application. Administration of 10 mg insulin-loaded MN arrays resulted in a markedly increased fall in BGL. However, the onset of action was slightly slower in comparison to that induced by 2.5 mg loaded MN arrays. A maximum BGL decrease of approximately 74% was observed after 4.7 h from the start of the experiment. The hypoglycaemic response induced by 10 mg insulin-loaded MN administered transdermally to diabetic rats was comparable to the effect produced by subcutaneous administration of the fresh insulin solution at a dose of 0.2 IU per animal. In MN-treated groups, BGL returned gradually to the initial values by 12 h of the experimental period. Statistical analysis revealed that there was statistical difference between the C_{max} induced by transdermal administration of insulin *via* 2.5 mg and 10 mg loaded MN arrays and the C_{max} produced by administration of fresh insulin solution ($p<0.05$ in both cases). No statistically significant difference was observed between the T_{max} of insulin transdermally delivered by 2.5 mg loaded PMVE/MA MN arrays to diabetic rats in comparison to the T_{max} of freshly prepared insulin solution ($p>0.05$). Statistical difference was found between the T_{max} of insulin transdermally delivered by

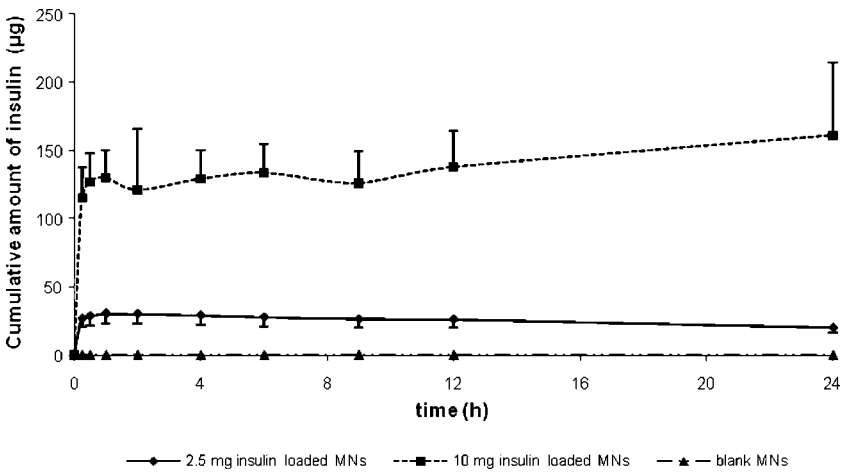

Fig. 4 *In vitro* release of insulin from MNs prepared from aqueous blends of 20% *w/w* PMVE/MA across dermatomed neonatal porcine skin (means ± SD, $n=5$).

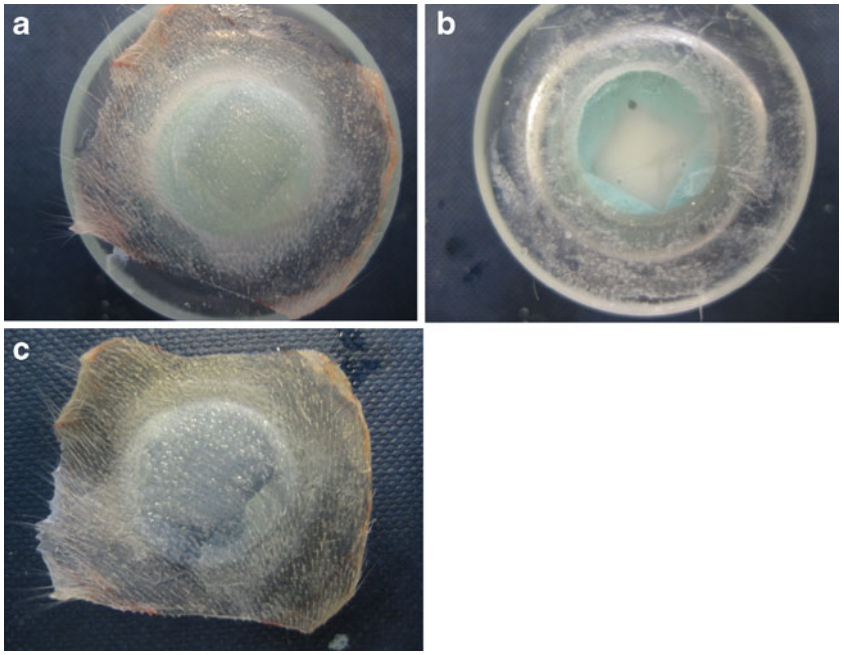

Fig. 5 Representative images of (**a**) underside of the dermatomed porcine skin, (**b**) remnants of the insulin loaded MN array, (**c**) *SC* side of the dermatomed porcine skin at the end of the 24 experimental period. Images were obtained with digital camera (Digital Ixus 75, Canon UK Ltd.).

10 mg loaded PMVE/MA MN arrays to diabetic rats in comparison to the T_{max} of freshly prepared insulin solution ($p<0.05$). No needles remained after removal from rat's skin at 24 h, indicating complete dissolution of the needles in the skin. MN array base-plates were found to be relatively intact, but with quite a degree of flexibility, due to moisture adsorption.

DISCUSSION

In the current study, the ability of MN arrays prepared from aqueous blends of 20% *w/w* PMVE/MA to increase skin permeability to a model macromolecule, insulin, was evaluated. Insulin was chosen as a model drug due to its clinical relevance. Each year, 5% of all deaths globally are caused by diabetes, according to WHO, and the main treatment in Type 1 diabetes, as well as in advanced stages of Type 2 diabetes, still remains hypodermic injection of insulin (24). Due to the pain and discomfort associated with insulin injections, as well as difficulty in mimicking physiological control of blood glucose levels, many attempts have been made to develop more convenient ways of insulin administration.

The transdermal route offers a range of advantages for delivery of peptide/protein therapeutics. As proteins have short plasma half-lives, the possibility of continuous delivery offered by the transdermal route is a major benefit, as is the low proteolytic activity in comparison to other routes (33). Furthermore, avoidance of first-pass hepatic metabolism eliminates another obstacle to successful systemic peptide/protein delivery. The major challenge associated with

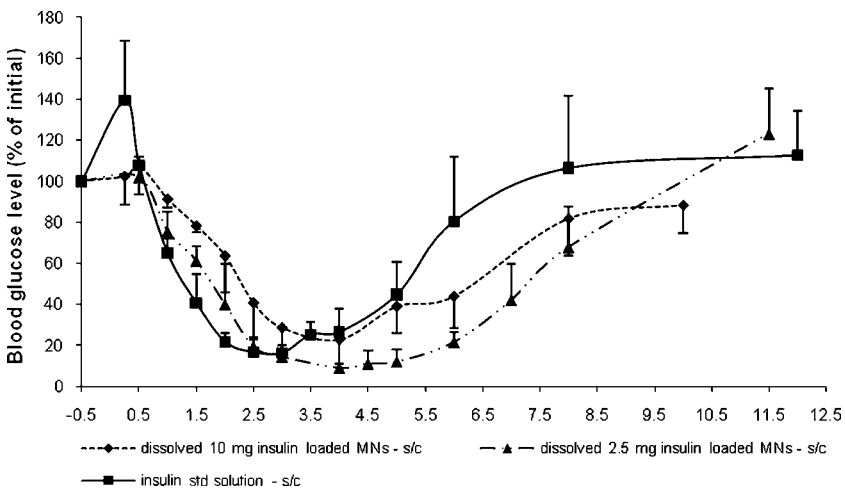

Fig. 6 Blood glucose levels as a percentage of the initial value in rats after subcutaneous administration of 1 ml of (♦) 0.2 IU/ml solution obtained by dissolving 10 mg insulin-loaded MN arrays prepared from aqueous blends of 20% *w/w* PMVE/MA (means ± SD, $n=4$), (▲) 0.2 IU/ml solution obtained by dissolving 2.5 mg insulin-loaded MN arrays prepared from aqueous blends of 20% *w/w* PMVE/MA (means ± SD, $n=5$), (■) freshly prepared 0.2 IU/ml insulin solution (means ± SD, $n=3$).

Table IV C_{max} and T_{max} Parameters of Insulin Recovered from MNs Prepared from Aqueous Blends of 20% *w/w* PMVE/MA and Subcutaneously Administered to Diabetic Rats and C_{max} and T_{max} Parameters of Subcutaneously Administered Freshly Prepared Insulin Solution

Formulation (dose 0.2 IU/ml)	C_{max} (%)	T_{max} (h)
dissolved 10 mg insulin loaded MNs	77.46 ± 11.8	4.0 ± 0.0
dissolved 2.5 mg insulin loaded MNs	92.02 ± 2.3	4.4 ± 0.5
fresh insulin solution	85.32 ± 1.8	2.67 ± 0.3

delivery of molecules across the skin is overcoming the *stratum corneum* barrier. Thus, a number of enhancement methods have been proposed and investigated to improve bioavailability of peptides/proteins administered transdermally, including chemical, electrical and physical methods such as penetration enhancers (25), drug carriers such as transfersomes (30) or biphasic lipid vesicles (31), iontophoresis (6,27), ultrasound (8,28), MNs (26,29,34,36), electroporation (7), thermal ablation (9) or radiofrequency ablation (32).

The present study highlighted the usefulness of MN arrays fabricated from aqueous blends of PMVE/MA as delivery platforms for biomolecules. The straightforward micromoulding process used in the present study to manufacture MN arrays was found to be suitable for encapsulation of potent therapeutics in the polymeric matrix. The employed preparation approach relying on casting aqueous PMVE/MA blends did not require harsh conditions, such as elevated temperatures, which could potentially destroy the fragile structure of biomolecules. A similar fabrication approach has been described by Lee *et al.* (17), where MN arrays were prepared by casting aqueous solutions of CMC and amylopectin into the micromoulds. This gentle process was applied to prepare CMC MNs encapsulating a model protein-lysozyme, and it was found that structural and functional integrity of the protein was retained after 2 months storage at room temperature (17). In addition, another gentle microfabrication process, which allowed encapsulation of active biomolecules within MN matrix, was developed by Sullivan *et al.* (37). Rapidly dissolving MNs were produced from monomeric vinyl pyrrolidone at room temperature using *in situ* photopolymerization process. It was found that the activity of ß-galactosidase was maintained after incorporation into the polymeric matrix. Conversely, Park *et al.* described fabrication of MNs during which drug was exposed to high temperatures (18). MNs encapsulating model protein-bovine serum albumin (BSA) were prepared out of poly-lactide-*co*-glycolide melted at 135°C. The substantial loss of BSA was reported after exposure of the drug to the hot polymer melt. Similarly, our previous study indicated that high processing temperature of galactose resulted in a complete degradation of BSA after incorporation into MN matrix (35).

The gentle nature of the method employed in the present MN fabrication process was mirrored in the insulin content analysis. Slight losses of insulin in comparison to the theoretical loading could be attributed to the potential interaction between deprotonated carboxyl groups of PMVE/MA polymer and charged amino acid residues of insulin. Alternatively, the discrepancy between theoretical and actual insulin loading could be explained by the potential interaction between the aqueous blend of 20% *w/w* PMVE/MA containing insulin and the mould. The storage of insulin-loaded MNs for 28 days at room temperature did not have an adverse effect on insulin stability, as confirmed by RP-HPLC analysis. Preservation of the original protein structure is necessary for its biological function; therefore, any alteration in the secondary conformation of protein may lead to loss of its biological activity or may render the protein immunogenic (38,39). Our results indicated that the secondary structure of insulin remained intact after incorporation into the matrix of MNs prepared from aqueous blends of PMVE/MA, as evidenced by the CD spectra, which were indistinguishable from that of insulin standard solution.

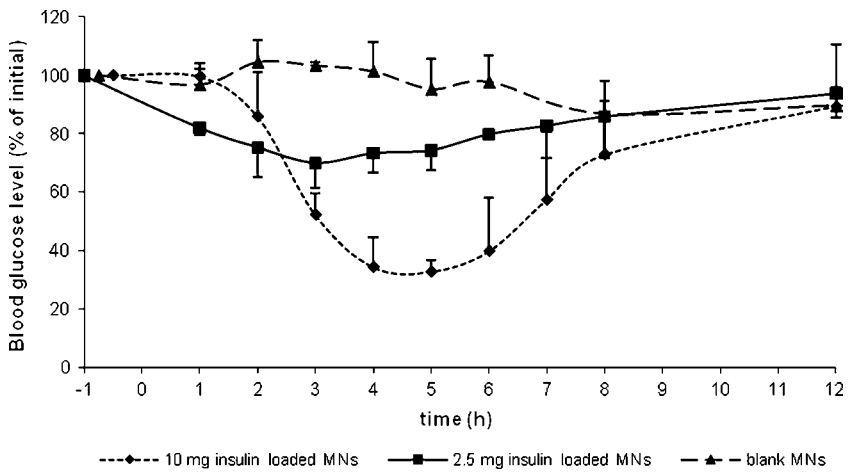

Fig. 7 Blood glucose levels as a percentage of the initial value in rats after transdermal application of (▲) 10 mg insulin-loaded MN arrays prepared from aqueous blends of 20% *w/w* PMVE/MA (means ± SD, $n = 3$), (■) 2.5 mg insulin-loaded MN arrays prepared from aqueous blends of 20% *w/w* PMVE/MA (means ± SD, $n = 3$) and (◆) non-insulin-loaded MN arrays prepared form aqueous blends of 20% w/w PMVE/MA (means ± SD, $n = 3$).

Table V C_{max} and T_{max} Parameters of Insulin Transdermally Administered with MN Arrays Prepared from Aqueous Blends of 20% *w/w* PMVE/MA to Diabetic rats and C_{max} and T_{max} Parameters of Freshly Prepared Insulin Solution Administered Subcutaneously

Formulation (dose 0.2 IU/ml)	C_{max} (%)	T_{max} (h)
10 mg insulin loaded MN array	73.54 ± 5.96	4.67 ± 1.15
2.5 mg insulin loaded MN array	32.41 ± 8.4	2.67 ± 0.58
fresh insulin solution	85.32 ± 1.8	2.67 ± 0.3

The final confirmation of the suitability of PMVE/MA matrix for encapsulation of insulin was provided by the *in vivo* assay where insulin released from MN arrays was subcutaneously injected into diabetic rats, with hypoglycaemic effects observed.

Composition of the MN matrix has been shown to affect the strength of MNs. Incorporation of drug substances into polymeric MN matrix could result in either a strengthening or weakening effect on MN mechanical strength, as reported by other authors (17,18). Encapsulation of insulin in the MN arrays prepared from aqueous blends of 20% *w/w* PMVE/MA did not affect their mechanical strength.

Insulin permeation from MN base-plates across dermatomed neonatal porcine skin was completely prevented (i.e. passive diffusion). In order to successfully permeate the *SC,* molecules should have intermediate lipophilicity (log P 1–3) and low molecular weight (less than 500 Da). Insulin as hydrophilic protein of a molecular weight of 5.6 kDa, clearly does not fulfil these criteria, which explains its poor diffusion across the neonatal porcine skin. The use of MNs prepared from aqueous blends of 20% *w/w* PMVE/MA and loaded with insulin markedly enhanced its delivery. It was observed that insulin release from the MN matrix exhibited a burst effect within the first 15 min of the experiment which was not followed by a significant increase in the amount of insulin delivered during the remaining of the study. The explanation of this observation could lie in the possibility that upon contact with the aqueous environment within the skin, needles of the MN array dissolved rapidly, releasing encapsulated insulin. However, further diffusion of the insulin from MN base-plates could be prevented by the dissolved polymeric matrix blocking the created microchannels as well as closure of the holes made by MN insertion. These assumptions could be supported by the fact that MN base-plates were transformed from the dried state into the mass of gel after 24 h on the skin and no MN holes were observed in the skin at the end of experiment. The cumulative amounts of insulin detected in the receptor compartment after 24 h accounted for only approximately 50% of the actual insulin amount present in the needles, which could be attributed to insulin entrapment in skin. The potential electrostatic interaction between extracellular skin components and insulin molecules could explain that hypothesis. Moreover, knowing insulin's tendency toward self-association and aggregation (40), formation of species larger than the insulin monomer could provide further explanation of the low insulin permeation across the skin. Insulin dimers and hexamers of molecular weight of 12 kDa and 36 kDa, respectively, are believed to be less mobile (41), which can result in poor skin diffusivity and mobility. The proteolytic degradation of insulin in the skin could be another potential factor affecting its transport across the skin. Huang and Wu observed significant degradation of insulin during iontophoresis, which, in addition to the electrochemical degradation and temperature, was attributed to the proteolytic degradation (42). On the contrary, Srinivasan *et al.* did not report insulin degradation in human skin at pH 7.4 under iontophoresis (43). In the present studies, proteolytic stability of insulin was not established. Therefore, in order to ascertain the contribution of insulin enzymatic degradation to its permeation across the skin in the *in vitro* scenario, additional studies are necessary.

Administration of insulin-loaded MNs prepared from aqueous blends of 20% *w/w* PMVE/MA to diabetic rats *in vivo* proved their usefulness in lowering BGL. A dose-dependent hypoglycaemic effect was observed following application of 2.5 and 10 mg loaded MN arrays to diabetic rats. Administration of 2.5 mg insulin-loaded MN arrays resulted in a slight drop, of approximately 30%, in BGL. The hypoglycaemic effect induced by administration of 10 mg insulin-loaded MN arrays to diabetic rats was comparable to the response produced by subcutaneous administration of the control solution. After removal of the MN array at the end of experiment no needles remained. Visual inspection of rat skin after removal of MNs revealed that no signs of skin irritation were present. As hypothesised above, most probably only insulin encapsulated within the needles was delivered. If the proposed hypothesis is valid, indirect comparison of insulin doses resulting in similar hypoglycaemic effects after administration *via* different routes could be achieved. The amount of insulin incorporated only into the needles of 10 mg insulin-loaded MN array was found to be approximately 0.29 mg, which is equivalent to 7.8 IU. The dose of subcutaneously administered control insulin solution was 0.2 IU. This indicated that approximately 40 times higher dose of insulin had to be delivered transdermally in order to obtain hypoglycaemic effect equivalent to that induced by subcutaneous injection. Although proteolytic activity of the skin is less pronounced in comparison to other routes of delivery, it can still pose an appreciable barrier for delivery of peptides and proteins. Therefore, in the present study, insulin delivered from MNs into the skin could be potentially degraded before reaching systemic circulation. Another

possible explanation of high transdermal dose of insulin necessary to induce hypoglycaemic effect in comparison to subcutaneous injection might be its interaction with skin components during transport through the skin to the microcirculation at the dermo-epidermal junction. During the transport through the skin, insulin might possibly associate with hydrophobic domains in the skin.

CONCLUSIONS

The present study demonstrated the feasibility of transdermal macromolecule delivery by means of dissolving polymeric MNs prepared from aqueous blends of 20% *w/w* PMVE/MA. The comparable effects on glucose levels between subcutaneous injection of insulin and 10 mg insulin-loaded polymeric MNs indicated that this strategy shows considerable potential for clinical therapy of diabetes. The current study shows that our novel polymeric MN device allows for the maintenance of structural integrity and biological activity of protein drugs and facilitates their rapid delivery across skin. In addition, the low cost of polymeric material as well as the ability to reuse micromoulds without altering the MN structure offers an inexpensive and reproducible method for the production of MNs. Approximately 10,000 MN arrays can be manufactured from 1 kg of PMVE/MA material with an estimated cost of 0.47 pence per array. Overall, our micromoulding technique allows for a low cost MN manufacture and, our MN delivery system could be applied for transdermal delivery of a variety of fragile biomolecules, including vaccines, in future clinical applications.

ACKNOWLEDGMENTS

This work was supported by BBSRC grant number BB/E020534/1.

REFERENCES

1. Brown L. Commercial challenges of protein drug delivery. Expert Opin Drug Del. 2005;2(1):29–42.
2. Kumar T, Soppimath K, Nachaegari S. Novel delivery technologies for protein and peptide therapeutics. Curr Pharm Biotechnol. 2006;7:261–76.
3. Banga AK. Therapeutic Peptides and Proteins: Formulation, Processing and Delivery Systems. Boca Raton: CRC Press; 2006.
4. Gupta H, Sharma A. Recent trends in protein and peptide drug delivery systems. Asian J Pharm. 2009;3(2):69–75.
5. Benson H, Namjoshi S. Proteins and peptides: Strategies for delivery to and across the skin. J Pharm Sci. 2008;97(9):3591–610.
6. Chaturvedula A, Joshi D, Anderson C, Morris R, Sembrowich W, Banga A. *In vivo* iontophoretic delivery and pharmacokinetics of salmon calcitonin. Int J Pharm. 2005;97(1–2):190–6.
7. Medi B, Singh J. Electronically facilitated transdermal delivery of human parathyroid hormone (1–34). Int J Pharm. 2003;263:25–33.
8. Park E, Werner J, Smith N. Ultrasound mediated transdermal insulin delivery in pigs using a lightweight transducer. Pharm Res. 2007;24(7):1396–401.
9. Badkar A, Smith A, Eppstein J, Banga A. Transdermal delivery of interferon alpha-2B using microporation and iontophoresis in hairless rats. Pharm Res. 2007;24:1389–95.
10. Fang JY, Lee WR, Shen SC, Wang HY, Fang CL, Hu CH. Transdermal delivery of macromolecules by erbium:YAG laser. J Control Release. 2004;100:75–85.
11. Prausnitz MR. Microneedles for transdermal drug delivery. Adv Drug Deliv Rev. 2004;56(5):581–7.
12. Kaushik S, Allen H, Donald D, McAllister D, Smitra S, Allen M, *et al.* Lack of pain associated with microfabricated microneedles. Anesth Analg. 2001;92:502–4.
13. Martanto W, Davis SP, Holiday NR, Wang J, Gill H, Prausnitz MR. Transdermal delivery of insulin using microneedles *in vivo*. Pharm Res. 2004;21(6):947–52.
14. Donnelly RF, Morrow DIJ, McCarron PA, Woolfson AD, Morrissey A, Juzenas P, *et al.* Microneedle-mediated intradermal delivery of 5-aminolevulinic acid: Potential for enhanced topical photodynamic therapy. J Control Release. 2008;129:154–62.
15. Matriano JA, Cormier M, Johnson J, Young WA, Buttery M, Nyam K, *et al.* Macroflux microprojection array patch technology: a new and efficient approach for intracutaneous immunization. Pharm Res. 2002;19(1):63–70.
16. Davis S, Martanto W, Allen M, Prausnitz M. Hollow metal microneedles for insulin delivery to diabetic rats. IEEE Trans Biomed Eng. 2005;52(5):909–15.
17. Lee JW, Park JH, Prausnitz MR. Dissolving microneedles for transdermal drug delivery. Biomaterials. 2008;29(13):2113–24.
18. Park JH, Allen MG, Prausnitz MR. Polymer microneedles for controlled-release drug delivery. Pharm Res. 2006;23(5):1008–19.
19. Park JH, Allen MG, Prausnitz MR. Biodegradable polymer microneedles: fabrication, mechanics and transdermal drug delivery. J Control Release. 2005;104:51–66.
20. Prausnitz MR, Langer R. Transdermal drug delivery. Nat Biotechnol. 2008;26(11):1261–8.
21. Donnelly RF, Majithiya R, Singh R, Morrow D, Garland M, Demir YK, *et al.* Design, optimization and characterization of polymeric microneedle arrays prepared by a novel laser-based micromoulding technique. Pharm Res. 2011;28(1):41–57.
22. Henricus M, Johnon K, Banerje I. Investigation of insulin loaded self-assembled microtubulus for drug release. Bioconjug Chem. 2008;19:2394–400.
23. Bouchard M, Zurdo J, Nettleton E, Dobson C, Robinson C. Formation of insulin amyloid fibrils followed by FTIR and simultaneously with CD and electron microscopy. Protein Sci. 2000;9:1960–7.
24. Owens DR, Zinman B, Bolli G. Alternative routes of insulin delivery. Diabet Med. 2003;20:886–98.
25. Karande P, Jain A, Mitragotri S. Discovery of transdermal penetration enhancers by high-throughput screening. Nat Biotechnol. 2004;22(2):192–7.
26. Ito Y, Saeki A, Shiroyama K, Sugioka N, Takada K. Percutaneous absorption of interferon-alpha by self-dissolving micropiles. J Drug Target. 2008;16(3):243–9.
27. Langkjaer L, Brange J, Grodsky GM, Guy R. Iontophoresis of monomeric insulin analogues in vitro: effects of insulin charge and skin pretreatment. J Control Release. 1998;51:47–56.
28. Tezel A, Sens A, Mitragotri S. Description of transdermal transport of hydrophilic solutes during low-frequency sonophoresis based on a modified porous pathway model. J Pharm Sci. 2003;92(2):381–93.

29. Ito Y, Ohashi Y, Saeki A, Sugioka N, Takada K. Antihyperglycemic effect of insulin from self-dissolving micropiles in dogs Chem. Pharm Bull. 2008;56(3):243–6.
30. Cevc G. Transdermal drug delivery of insulin with ultradeformable carriers. Clin Pharmacokinet. 2003;42(5):461–74.
31. King M, Badea I, Solomon J, Kumar P, Gaspar K, Foldvari M. Transdermal delivery of insulin from novel biphasic lipid system in diabetic rats. Diab Technol The. 2002;4(4):479–88.
32. Levin G, Gershonowitz A, Sacks H, Stern M, Sherman A, Rudaev S, *et al.* Transdermal delivery of human growth hormone through RF-microchannels. Pharm Res. 2005;22(4):550–5.
33. Banga A. Theme section: Transdermal delivery of proteins. Pharm Res. 2007;24(7):1357–9.
34. Ito Y, Yamazaki T, Sugioka N, Takada K. Self-dissolving micropile array tips for percutaneous administration of insulin. J Mater Sci Mater M. 2010;21:835–41.
35. Donnelly RF, Morrow DIJ, Thakur RRS, Migalska K, McCarron PA, O'Mahony C, *et al.* Processing difficulties and instability of carbohydrate microneedle arrays. Drug Dev Ind Pharm. 2009;35:1242–54.
36. Ito Y, Eiji H, Atsushi S, Nobuyuki S, Kanji T. Feasibility of microneedles for percutaneous absorption of insulin. Euro J Pharm Sci. 2006;29(1):82–8.
37. Sullivan SP, Murthy N, Prausnitz MR. Minimally invasive protein delivery with rapidly dissolving polymer microneedles. Adv Mater. 2008;20:933–8.
38. Wangoo N, Suri C, Shekawat G. Interaction of gold nanoparticles with protein: A spectroscopic study to monitor protein conformational changes. App. Phys. Lett. 2008;92(13) ID 133104
39. Brandes N, Welzel P, Werner C, Kroh L. Adsorption-induced conformational changes of proteins onto ceramic particles: Differential scanning calorimetry and FTIR analysis. J Colloid Interf Sci. 2006;299(1):56–69.
40. Lougheed WD, Woulfe-Flanagan H, Clement JR, Albisser A. Insulin aggregation in artificial delivery systems. Diabetologia. 1980;19:1–9.
41. Pillai O, Borkute S, Sivaprasad N, Panchagnula R. Transdermal iontophoresis of insulin II. Physicochemical considerations. Int J Pharm. 2003;254:271–80.
42. Huang Y, Wu S. Stability of peptides during iontophoretic transdermal delivery. Int J Pharm. 1996;131:19–23.
43. Srinivasan V, Higuchi W, Sims S, Ghanem A, Behl C. Transdermal iontophoretic drug delivery: Mechanistic analysis and application to polypeptide delivery. J Pharm Sci. 1989;78(5):370–5.
44. International conference on harmonisation of technical requirements for registration of pharmaceuticals for human use, ICH harmonised tripartite guideline—Validation of Analytical Procedures: Text and Methodology—Q2(R1), 2005
45. Kadima W, Ogendal L, Bauer R, Kaarsholm N, Brodersen K, Hansen JF, *et al.* The influence of ionic strength and pH on the aggregation properties of zinc-free insulin studied by static and dynamic laser light scattering. Biopolymers. 1993;33(11):1643–57.
46. Tokumoto S, Higo N, Sugibayashi K. Effect of electroporation and pH on iontophoretic transdermal delivery of human insulin. Int J Pharm. 2006;326:13–9.
47. Sadhale Y, Shah J. Biological activity of insulin in GMO gels and the effect of agitation Int. J Pharm. 1999;191:65–74.